Indonesian Journal of Biotechnology

VOLUME 27(4), 2022, 203-211 | RESEARCH ARTICLE

Anti-diabetic effect of andrographolide from Sambiloto herbs (*Andrographis paniculata* (Burm.f.) Nees) through the expression of *PPARγ* and *GLUT-4* in adipocytes

Novia Tri Astuti[1], Putri Rachma Novitasari[1], Raymond Tjandrawinata[2], Agung Endro Nugroho[3,*], Suwijiyo Pramono[4]

[1]Master Program of Pharmaceutical Sciences, Faculty of Pharmacy, Universitas Gadjah Mada, Yogyakarta 55281, Indonesia
[2]Dexa Laboratories of Biomolecular Sciences (DLBS), Cikarang 17550, Indonesia
[3]Department of Pharmacology and Clinical Pharmacy, Faculty of Pharmacy, Universitas Gadjah Mada, Yogyakarta 55281, Indonesia
[4]Department of Pharmaceutical Biology, Faculty of Pharmacy, Universitas Gadjah Mada, Yogyakarta 55281, Indonesia
*Corresponding author: agungendronugroho2020@yahoo.com

SUBMITTED 31 August 2021 **REVISED** 28 April 2022 **ACCEPTED** 27 July 2022

ABSTRACT Andrographolide has been shown to have a pharmacological effect as an antidiabetic. Nevertheless, the comprehensive mechanism of action has yet to be determined. Andrographolide is a primary component of the sambiloto herb (*Andrographis paniculata* (Burm.f.) Nees), in which a simple isolation process can obtain high yields. This study aimed to explain the anti-diabetic effect of andrographolide compared to pioglitazone (a positive control) on glucose uptake by measuring the expression levels of peroxisome proliferator-activated receptor gamma (*PPARγ*) and glucose transporter type 4 (*GLUT-4*) genes in 3T3-LI mouse adipocytes as an *in vitro* model. The differentiation of mature adipocytes from 3T3-L1 fibroblasts was induced with 3-isobutyl-1-methylxanthine, dexamethasone, and insulin. Andrographolide was provided through direct isolation from *A. paniculata* herbs. The gene expression was detected using the reverse transcription-polymerase chain reaction (RT-PCR). Pioglitazone and andrographolide significantly increased glucose uptake capability. Andrographolide was able to increase the mRNA levels of *PPARγ* and *GLUT-4* compared to pioglitazone with the best concentration at 5.6 µM. In conclusion, andrographolide can improve glucose uptake by increasing mRNA levels of *PPARγ* and *GLUT-4* that encodes protein, which are key factors for glucose homeostasis. Therefore, this finding further establishes the potency of andrographolide from *A. paniculata* as an antidiabetic.

KEYWORDS 3T3-L1 adipocytes; andrographolide; glucose uptake; *PPARγ*; *GLUT-4*

1. Introduction

In 2019, the International Diabetes Federation (IDF) estimated that 483 million people worldwide suffer diabetes mellitus (DM) with a prevalence of 9.3%. According to the IDF, diabetic patients will rise to 578 million in 2030 and 700 million in 2045. Among them, type 2 DM is the most common case, recorded in as much as 90% of all diabetes cases globally (Zheng et al. 2018). Obesity is a condition that is intimately correlated to the occurrence of type 2 DM and other metabolic diseases. At the cellular level, obesity is defined by a rise in the size and amount of adipocytes in adipose tissue (Al-Goblan et al. 2014). Obesity-related adipose tissue failure to adequately store excess energy resulted in ectopic lipid deposition, decreased insulin sensitivity (resistance), and eventually type 2 DM (Chait and den Hartigh 2020). Insulin is essential for maintaining glucose homeostasis in skeletal muscles, adipose tissue, and the liver. Insulin resistance is characterized by a reduced sensitivity and response to metabolic activation of the insulin receptor, and it is linked to several metabolic diseases and hemodynamic disruptions (Shoelson et al. 2006).

Peroxisome proliferator-activator receptor gamma (*PPARγ*) has tissue-specific effects that are most prominent in adipose tissue. *PPARγ* regulates the expression of adipocyte-secreted factors in adipose tissue (Ahmadian et al. 2013). *PPARγ* activation increases fatty acid uptake and sequestration in adipose tissue, improves insulin sensitivity, and eventually upregulates glucose uptake genes (Hauner 2002; Sugii et al. 2009; Gandhi et al. 2013). As a result, adipose tissue is a critical therapeutic target for treating insulin resistance of type 2 DM.

Insulin sensitivity can be improved with drugs that primarily act as activators of *PPARγ*, such as thiazolidinediones (TZDs), i.e., pioglitazone and rosiglitazone. The treatment with TZDs influenced and changed the expression of signaling molecules of the insulin signaling cascade (insulin receptor substrate (*IRS*),

phosphatidylinositol-3-kinase (*PI3K*), protein kinase-B (*PKB/Akt*), endothelial nitric oxide synthase (*eNOS*), 5-AMP kinase, glucose transporter type 4 (*GLUT-4*)) connected with improvement of insulin sensitivity and endothelial dysfunction (Fasshauer et al. 2000; Ahmadian et al. 2013; Sugii et al. 2009; Kvandová et al. 2016). *PPARγ* activation through binding by TZDs will improve insulin sensitivity, increase the rate of glucose transporter type 4 (*GLUT-4*) synthesis and translocate *GLUT-4* to the cell plasma membrane, which will help control blood sugar levels (Wang et al. 2016). TZDs have been implicated in various side effects, including typical weight gain, peripheral edema, and a higher risk of cardiac hypertrophy (Basu et al. 2006; Horita et al. 2015). Side effects have been observed in synthetic drugs. Hence, traditional medicines are evolving as viable options.

Efforts to develop traditional medicines are still very interesting and challenging, including extracts (Fajrin et al. 2020; Wigati et al. 2017), fractions (Harwoko et al. 2014), and isolates (Nugroho et al. 2011) from plants. Andrographis paniculata is a medicinal plant that has long been used in Asia to treat various ailments. Antioxidant (Rafat et al. 2010), hepatoprotective (Maiti et al. 2010), anticancer (Malik et al. 2021), antimalaria (Widyawaruyanti et al. 2014), and antihyperglycemic (Nugroho et al. 2012) are some of the pharmacological effects of this herb. Andrographolide is the key compound found in *A. paniculata*. Nugroho et al. (2013) found that the andrographolide-enriched extract from *A. paniculata* herb reduces blood glucose levels and improves pancreatic beta cells in streptozocin-induced diabetic rats. The influence of andrographolide has been shown to improve insulin sensitivity by increasing glucose uptake, activating insulin signaling, and suppressing the signaling activation of nuclear factor kappa-B (*NF-κB*) by tumor necrosis factor-alpha (*TNF-α*) in 3T3-L1 cells (Jin et al. 2011). Furthermore, andrographolide has been shown to suppress *PPARγ* expression in the early stages of differentiation, inhibiting 3T3-L1 cells differentiation into mature adipocytes; as a result, it has the potential to treat obesity and diabetes conditions (Jin et al. 2012). Recently, a study reported that a combination fraction of *A. paniculata* herb and *Centella asiatica* herb increased the expression of the *PPARγ* and *GLUT-4* genes in 3T3 L1 adipocytes with resistance insulin (Fitrawan et al. 2018). Aside from these findings, the essential role of andrographolide in anti-diabetic activity and the underlying mechanisms remain unknown.

In our previous study, the isolated andrographolide from the *A. paniculata* at the concentrations of (0.8-7 µM (LC_{50}=10.771 µM) did not lead to cell toxicity in 3T3-L1 pre-adipocytes (Novitasari et al. 2020). Therefore, this study aimed to investigate the effect of andrographolide, isolated from *A. paniculata* on glucose uptake concerning the expression of *PPARγ* and *GLUT-4* at mRNA levels.

2. Materials and Methods

2.1. Cell culture

Swiss albino 3T3-L1 fibroblasts obtained from the American Type Culture Collection (ATCC® CRL-1658TM, Manassas, VA) were cultured in DMEM (Dulbecco's Modified Eagle Medium) growth medium containing high glucose (12800058, Gibco) supplemented with 10% bovine serum (BS) (16170078, Gibco) and 1% penicillin/streptomycin (P/S) (15140148, Gibco), and were incubated at 37 °C in a humidified atmosphere of 5% CO_2. The cells were then sub-cultured every 2-3 days on a 100-mm petri dish with an estimated 90% confluence.

2.2. Adipocyte differentiation

3T3-L1 pre-adipocytes differentiation was carried out by replacing the cell growth medium with another medium containing DMEM (high glucose), 10% fetal bovine serum (FBS) (26140095, Gibco), and MDI cocktail (IBMX (3-isobutyl-1-methylxanthine) 0.25 µM (I7018, Sigma Aldrich), dexamethasone 0.25 µM (D1756, Sigma Aldrich), and insulin 1 µg/mL (I0305000, Sigma Aldrich). The cell density was about 1×10^4 cells/mL in a 35-mm petri dish. On the third day, the medium was changed to one containing high glucose of DMEM, 10% FBS, 1% P/S, and 1 µg/mL insulin (I0305000, Sigma Aldrich). The cells were maintained for up to ten days, and the medium was changed every two to three days. Early adipocytes were observed by measuring the expression of adiponectin and *C/EBPα* genes, while mature adipocytes were observed by oil-red o (ORO) staining.

2.3. Oil red O (ORO) staining

Cells were harvested on the tenth day after differentiation, and lipid accumulation was measured using ORO staining as proof of cell differentiation. ORO solution is prepared by dissolving 0.7 g of ORO powder (O0625, Sigma Aldrich) in 200 mL of 100% isopropanol (107022, Merck) stirred overnight, then was filtered through a 0.22 µM membrane and kept at 4 °C in a dark. The cells on the dish were washed three times with phosphate-buffered saline (PBS)-10×, then 1 mL of 10% formalin (47608, Sigma Aldrich) was added. The cells were incubated for 1 h or more at room temperature. After removing the formalin, the cells were washed with 60% isopropanol and air-dried at room temperature. The cells were incubated at room temperature for 10 min after adding ORO solution. The ORO solution was discarded and the cells were washed with ddH_2O. The cells were then observed under a microscope to identify the lipid droplets. The accumulation of colored lipids was quantified by spectrophotometer at 520 nm by adding 1 mL of 100% isopropanol to the cells for each dish.

2.4. Treatment of andrographolide

The isolated andrographolide was obtained from the isolation of *A. paniculata* by Novitasari et al. (2020). The

isolated andrographolide and positive control (pioglitazone (C30277, Sigma Aldrich) was dissolved with DMSO 0.03% (1029524000, Merck). Before administering the treatment, the medium was changed into a serum-free DMEM medium. The andrographolide isolate (1.4, 2.8, and 5.6 µM), positive control (pioglitazone 0.02 µM), and negative control (DMSO 0.03%) were administered on mature adipocytes in the serum-free DMEM medium and incubated for 24 h at 37 °C incubator with 5% CO_2 aeration. Crude extract of *A. paniculata* (30 µg/mL) was also provided to 3T3-L1 cells separately to compare its effect to the active isolate.

2.5. RNA extraction

Total RNA of 3T3-L1 cells was extracted using Ribo-Ex™ reagent (302001, GeneAll). Briefly, 3T3-L1 cells were lysed in the reagent before being extracted with chloroform (102444, Merck) and precipitated with 2-propanol (107022, Merck) at 4 °C. Ethanol 75% (108543, Merck) was used to wash off the rest of the reagent. Prior to use, the pellet was suspended in nuclease-free water (NFW) (P1193, Promega) and stored at -20 °C. The RNA concentration and purity level (A260/280) were determined using the NanoDrop 2000c spectrophotometer (Thermo Fisher Scientific, USA) at 260 and 280 nm. The absorbance at 260 nm determines the total nucleic acid content, whereas the absorbance at 280 nm determines the purity of the sample. The yield ratio A260/280 2.0 was considered pure.

2.6. cDNA synthesis

The RNA (1 µg) was reverse transcripted into cDNA using ReverTra Ace®qPCR RT Master Mix (FSQ201, Toyobo) according the manufacturer protocol. Briefly, the RNA was incubated for 5 min at 65 °C. The reverse transcription formula was carried out in a total volume of 10 µL of 1 µg RNA, 2 µL of 5× RT master mix, 0.5 µL of 5× RT master mix no RT-control, and NFW. The reaction was proceeded at 37 °C for 15 min and heated to 98 °C for 5 min. Prior to use, the cDNA as the reverse transcription product was stored at -20 °C.

2.7. Polymerase chain reaction (PCR)

Polymerase chain reaction (PCR) was used to analyze genes that play a role in adipocyte differentiation (adiponectin and *C/EBPα*) and antidiabetic effect through upregulation of *PPARγ* and *GLUT-4* expressions. Table 1 shows nucleotide sequences of primers used for PCR. The gene amplification reaction was carried out in a 25 µL reaction containing 12.5 µL Go Taq Green master mix (M7122, Promega), a pair of primer target genes at a final concentration of 1 µM, a pair of internal controls (*β-actin*) at a final concentration of 0.2 µM, 3 µL of cDNA, and NFW. The PCR conditions for each target gene are the same and generally consist of initial denaturation for 5 min at 95 °C, followed by 30-35 cycles of denaturation at 95 °C for 30 seconds, primer annealing at 58-60 °C for 30 seconds, and elongation at 72 °C for 10 min. The T3000 Thermocycler (BiometraPCR) was used. PCR samples were electrophoresed using agarose gel containing ethidium bromide (1558011, Invitrogen) and detected using a UV lamp on GelDoc (Biorad). Band intensity was determined using analysis Image J (National Institutes of Health, Bethesda, MD; v 1.24) and adjusted for *β-actin*.

2.8. Glucose uptake assay

The ratio of total glucose administered to glucose levels obtained after incubation was used to calculate glucose uptake. The amount of glucose that reacts with anthrone in concentrated sulfuric acid is calculated to determine the glucose levels. The anthrone reagent (1014680010, Merck), was prepared by dissolving it in 75% H_2SO_4 (1007312511, Merck). After incubating for at least 2 h the reagent was ready and can be used within 24 h.

On 6-well plates, pre-adipocytes and mature adipocytes were grown to approximately 1×10^4 cells/mL and maintained in a growth medium containing high glucose DMEM containing 10% FBS and 1% P/S. After 80% confluence, the cells were treated with DMSO 0.03% (negative control), pioglitazone 0.02 µM (positive control), and andrographolide at the concentrations of 1.4; 2.8; and 5.6 µM for 24 h, incubated at 37 °C in

TABLE 1 Primers used to amplify the region of interest in PCR

Gene names	Primer sequences	PCR product (bp)
Adiponectin	F: 5'-CCCTTGCTTTTTGCACCTCC-3' R: 5'-AATCCTTGGCCCTCTGAGAT-3'	192
C/EBPα	F: 5'-CCCTTGCTTTTTGCACCTCC-3' R: 5'-GCTTTCTGGTCTGACTGGGG-3'	118
PPARg	F: 5'-TTCTCAAGGGTGCCAGTTTC-3' R: 5'-AATCCTTGGCCCTCTGAGAT-3'	198
GLUT-4	F: 5'-ACTCTTGCCACACAGGCTCT-3' R: 5'-AATGGAGACTGATGCGCTCT-3'	174
β-actin (internal control)	F: 5'-ACCCACACTGTGCCCATCTA-3' R: 5'-CGCAACCGCTCATTGCC-3'	289

Abbreviations: PCR, polymerase chain reaction; F, Forward sequence; R, Reverse sequence; *C/EBPα*, CCAAT/enhancer-binding protein-α; *PPARγ*, peroxisome proliferator activated receptor gamma; *GLUT*-4, glucose transporter type 4.

a humidified atmosphere of 5% CO_2. The media was discarded the next day, and the cells were washed three times with PBS-10×. Furthermore, in each treatment, the cells were given 2 mL of DMEM (no glucose) with an additional 200 µg/mL d-glucose (G8270, Merck), incubated at 37 °C in a humidified atmosphere of 5% CO_2, and sampled by taking 100 µL (duplo) of each well at 2, 4, 6, and 8 h. These cells can consume glucose during incubation, allowing the remaining sugar in the media to be measured, as well as the glucose level. After sampling, 100 µL of 75% H_2SO_4 and 400 µL anthrone reagent were added to each tube sample. The tube was incubated for 15 min in a 100 °C water bath before being placed in a dark room for few minutes. A spectrophotometer (BioRad) set to 625 nm was used to measure the optical density. A linear regression equation based on the standard curve between the glucose concentration in the medium and the absorbance generated at 625 nm was used to calculate the percentage of glucose uptake. The following equations were used to calculate the amount of glucose consumed by the cell.

Glucose uptake

$$= (Initial\ glucose - Residual\ glucose\ in\ the\ medium) \quad (1)$$

% Glucose uptake

$$= \frac{(Initial\ glucose - Residual\ glucose\ in\ the\ medium)}{Initial\ glucose} \times 100\% \quad (2)$$

2.9. Statistical analysis

Data are shown as mean ± standard error (SE). IBM SPSS Statistic for Macintosh version 25 was used to conduct the statistical analysis. The data obtained were analyzed with one-way ANOVA and continued with the least significant difference (LSD) post hoc test. The significance value was set at $p < 0.05$.

3. Results and Discussion

3.1. Expression of C/EBPα, adiponectin, PPARγ, and GLUT-4 during 3T3-L1 adipocytes differentiation

Differentiation of adipocytes consists of stages, i.e., pre-adipocytes, early adipocytes, mature adipocytes, and advanced adipocytes (Fajas 2003). Following induction with an MDI cocktail, 3T3-L1 fibroblasts can differentiate into lipid-laden adipocytes in about one week. The cocktail triggered the adipogenicity program and directed them to various stages of adipogenesis (Sarjeant and Stephens 2012). Mature adipocytes were used in this study to assess isolated andrographolide. *C/EBPα* and adiponectin, two genes involved in early differentiation, and *PPARγ* as well as *GLUT-4*, genes involved in the terminal stages of differentiation and glucose homeostasis, were observed in this experiment.

The early adipocytes stage emerges within three days of removing the MDI media. Figure 1a showed that adiponectin expression increased 1.5-fold compared to pre-adipocytes ($p < 0.05$). In addition, the increase in *C/EBPα* expression in early adipocytes was 1.7-fold higher than in pre-adipocytes ($p < 0.05$), as shown in Figure 1b. After ten days of differentiation, mature adipocytes were formed in this study. *PPARγ* was 1.7-fold more expressed in mature adipocytes than in pre-adipocytes ($p < 0.05$), as shown in Figure 1c. Furthermore, *GLUT-4* expression was increased in mature adipocytes 1.4-fold more than in pre-adipocytes ($p < 0.05$) (Figure 1d).

Substantial evidence suggests that *PPARγ* and *C/EBPα* are master regulators of adipocyte formation and differentiation, and adipogenesis (Lefterova et al. 2008). The expression of functional *PPARγ* was required for adipogenesis both *in vitro* and *in vivo*. During the early stages of differentiation, *C/EBPδ* and *C/EBPβ* are expressed at high levels in response to hormonal induction to trans-activate *C/EBPα* and *PPARγ* (Moseti et al. 2016). Activation of *PPARγ* and *C/EBPα* drives cells toward terminal differentiation and induces the expression of adipocyte-specific genes such as adiponectin, *GLUT-4*, and lipoprotein lipase (*LPL*) (Sarjeant and Stephens 2012; Moseti et al. 2016; Fan et al. 2019). According to Fu et al. (2005), adiponectin promotes cell proliferation, is involved in adipogenesis, enhances lipid content, and improves the insulin sensitivity of the glucose transport system in adipose tissues.

3.2. Oil Red O (ORO) staining on 3T3-L1 cells

The differentiation of pre-adipocytes into adipocytes was also assessed based on increased synthesis and accumulation of lipid in the cells. Staining techniques, such as lipid droplet (LD) staining with ORO reagent, are used *in vitro* to analyze these cells (Fan et al. 2019). Adipocytes will stain red after ORO staining, with optical density increasing linearly based on the number of lipid accumulation.

The experiments revealed that mature adipocytes accumulated lipid 3-fold greater than pre-adipocytes ($p < 0.05$) and 2.3-fold greater than early adipocytes ($p < 0.05$). In contrast, the early adipocytes only gave 1.4-fold greater than pre-adipocytes ($p < 0.05$). Figure 2 depicts the morphological appearance of 3T3-L1 cells after ORO staining.

3.3. Profile of glucose uptake in pre-adipocytes and mature adipocyte cells

The following preliminary test was performed to assess the difference in glucose uptake ability between pre-adipocytes and mature adipocytes in normal and solvent-induced (DMSO 0.03%). The onset of glucose absorption in mature adipocytes was earlier than in pre-adipocytes (Figure 3a). The percentage of glucose absorption in both cells had steadily increased over time. Pre-adipocytes and mature adipocytes had 61.75% and 73.71% glucose uptake capacities at the eighth hour, respectively ($p < 0.05$). In addition, DMSO-induced mature adipocytes had a glucose uptake capacity of 67.82%, which was lower than that of mature adipocytes ($p < 0.05$). This data suggests that DMSO indirectly reduced the ability of mature adipocytes to take up glucose. Mature adipocytes-DMSO induced

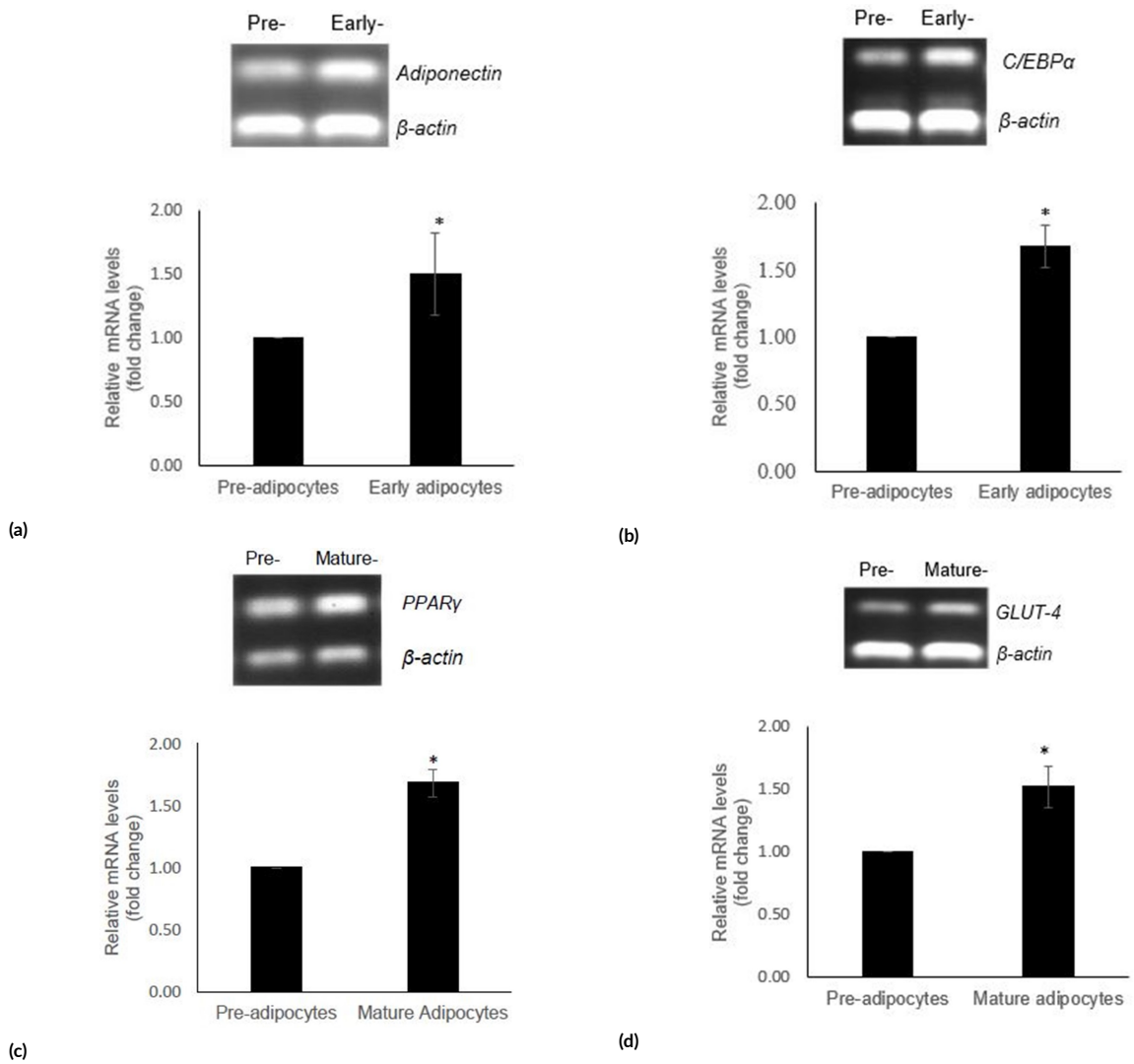

FIGURE 1 Expression genes during 3T3-L1 cells differentiation. (a) Adiponectin mRNA levels in early adipocytes. (b) *C/EBPα* mRNA levels in early adipocytes. (c) *PPARγ* mRNA levels in mature adipocytes. (d) *GLUT-4* mRNA levels in mature adipocytes. Results are mean values ± SE (n=3). *$p < 0.05$ indicates a significant difference in comparison to this of pre-adipocytes (control).

will be used as negative controls in the study.

In previous research by Tjandrawinata et al. (2011), the percentage of glucose uptake in mature adipocytes was higher than in pre-adipocytes. Our findings suggested that mature adipocytes modeling was adequate, as the percentage of glucose absorption in mature adipocytes was higher than in pre-adipocytes ($p < 0.05$). As shown in Figure 1, *PPARγ* and *GLUT-4* expression were increased in mature adipocytes, implying that *PPARγ* activation in the terminal stage resulted in increased expression of adipocyte-specific marker genes such as *GLUT-4*. Increased *GLUT-4* expression increases glucose uptake and insulin sensitivity (Fu et al. 2005; Wang et al. 2016).

3.4. Effect of andrographolide on glucose uptake

The glucose absorption capacity of the research sample was tested on mature adipocytes in this experiment. Glucose uptake capacity of andrographolide (1.4, 2.8, 5.6 µM) and pioglitazone (0.02 µM) in mature adipocytes was shown in Figure 3b. The experiment demonstrated that absorption occurs in all groups within 2 h of treatment and that the longer the treatment, the greater the absorption (2-8 h). All groups experienced an increase in glucose uptake capacity compared to the DMSO 0.03% (negative control). However, after 2 h of treatment, both the andrographolide group and the positive control (pioglitazone) showed negligible absorption potential. The maximum absorption capacity at 8 h in the positive control (pioglitazone 0.02 µM) was 92.71%, while the andrographolide treatment group 1.4, 2.8, and 5.6 µM were 83.97%, 93.85%, and 98.89%, respectively ($p < 0.05$). This study suggested that the isolated andrographolide provides similar capabilities to pioglitazone in inducing glucose uptake activity.

3.5. Effect of andrographolide on PPARγ and GLUT-4 expression

The experiment was carried out by calculating *PPARγ* and *GLUT-4* mRNA levels in mature adipocytes from the test

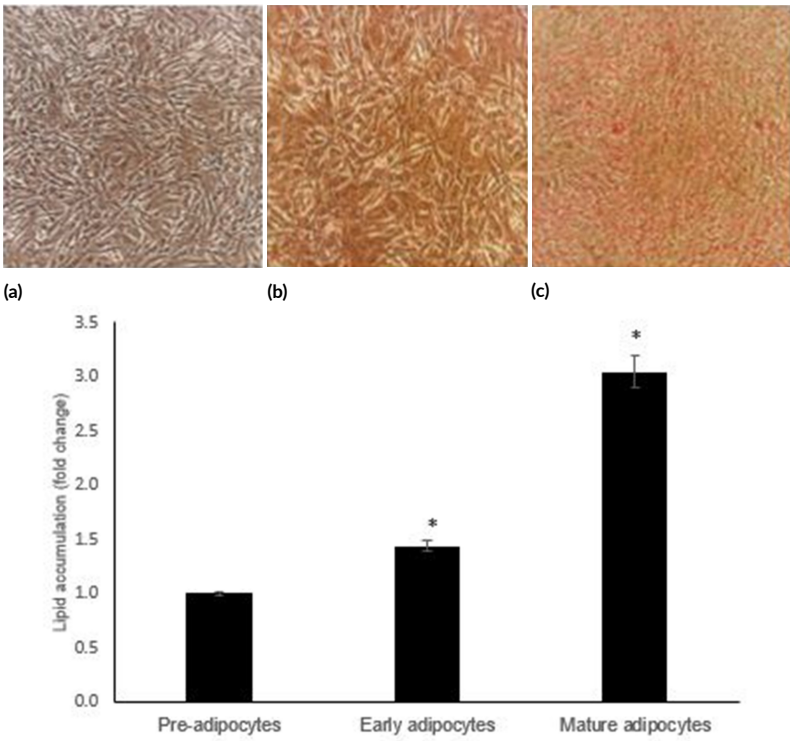

FIGURE 2 ORO staining assay. The morphological appearance of 3T3-L1 cells was observed under the microscope at 4×10 magnification after ORO staining. Increased ORO-stained cells are associated with pre-adipocytes differentiation into mature adipocytes due to lipid accumulation. (a) Pre-adipocytes. (b) Early adipocytes. (c) Mature adipocytes. Results are mean values ± SE (n=3). *p < 0.05 indicates a statistically significant difference in comparison to that of control cells.

sample. Figure 4 showed that *PPARγ* and *GLUT-4* mRNA levels increased in all treatment groups after treatments in mature adipocytes compared to the control. The administration of andrographolide 1.4 µM resulted in a 1.1-fold increase in *PPARγ* expression compared to DMSO 0.03% (negative control) ($p > 0.05$). Andrographolide 2.8 and 5.6 µM increased *PPARγ* expression by 1.3-fold and 1.8-fold, respectively, compared to DMSO 0.03% (negative control) ($p < 0.05$). The experiment was also carried out on the crude extract of *A. paniculata* herbs, in which *PPARγ* levels enhanced 1.3-fold compared to DMSO 0.03% ($p < 0.05$). The positive control (pioglitazone 0.02 µM) gave an increase of *PPARγ* expression 1.4-fold higher than the negative control ($p < 0.05$). Figure 4a displays all of the data.

Meanwhile, administration of 1.4, 2.8, and 5.6 µM andrographolide, respectively, increased *GLUT-4* expression by 2.4-fold, 2.7-fold, and 2.9-fold compared to DMSO 0.03% ($p < 0.05$). In comparison, the provision of crude extract provided an increase of only 1.2-fold compared to DMSO 0.03% (negative control) ($p < 0.05$). Pioglitazone 0.02 µM showed an increase of *GLUT-4* expression by 1.5-fold greater than DMSO 0.03% ($p < 0.05$). All of the data is shown in Figure 4b. These findings show that andrographolide administration increased *GLUT-4* and *PPARγ* expression significantly more than pioglitazone and crude extract ($p < 0.05$). This proved that andrographolide is responsible in upregulating *PPARγ* and *GLUT-4* expression. Andrographolide may influence the *PPARγ* pathway and stimulate glucose uptake.

One of the types of DM therapy is the oral drug thiazolidinediones (TZDs) class, such as rosiglitazone and pioglitazone. TZDs are *PPARγ* agonists that act as insulin sensitizers in treating DM type 2 with insulin resistance (Soccio et al. 2014). *PPARγ*, downregulated during tissue insulin resistance, is the molecular target for treating type 2 diabetes. In addition, activation of *PPARγ* alters the transcription of several genes involved in lipid and glucose metabolism, including those encoding lipoprotein lipase, adipocyte fatty acid-binding protein, fatty acid transporter protein, glucokinase, fatty acyl-CoA synthase, and *GLUT-4* (Cignarelli et al. 2013; Blanchard et al. 2016; Pereira et al. 2019). However, these agonists of *PPARγ* are associated with various side effects, including weight gain, fluid retention, edema, and congestive heart failure (Ahmadian et al. 2013; Horita et al. 2015).

Glucose transporter (*GLUT*) activation is critical in the insulin signaling cascade, resulting in effective glucose disposal into peripheral tissues. The two integral isoforms of glucose transporter proteins found in adipose tissue, *GLUT-1* and *GLUT-4*, regulate body glucose homeostasis and play a role in tissue glucose uptake. Glucose transporter type 1 (*GLUT-1*) participates in low intensity of glucose uptake. Glucose transporter type 4 (*GLUT-4*) plays the primary role in regulating glucose homeostasis through translocation and activation, subsequently triggered by the insulin-dependent PI3K/Akt pathway (Cao et al. 2010; Gandhi et al. 2013; Bao et al. 2020). Further-

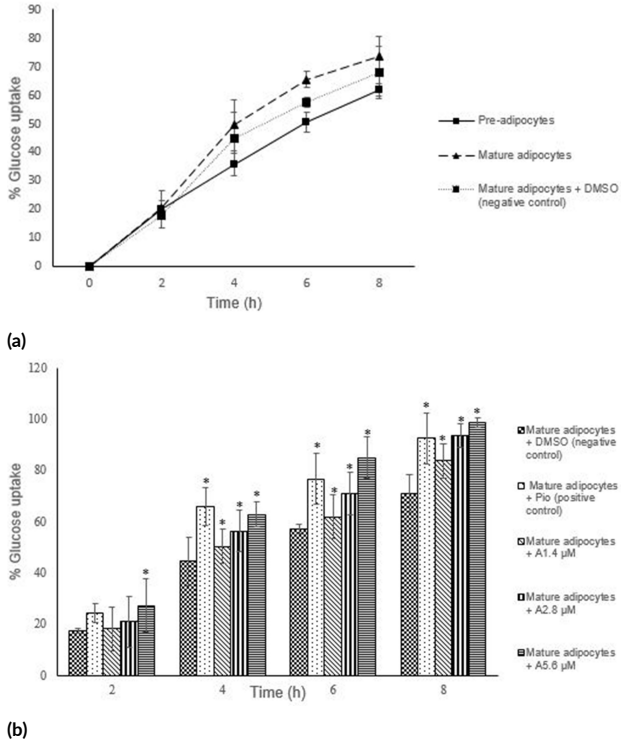

FIGURE 3 Andrographolide increases glucose uptake in mature adipocytes. (a) Profile of glucose uptake on pre-adipocytes and mature adipocytes and negative control (mature adipocytes + DMSO 0.03%). (b) Glucose uptake levels in mature adipocytes respond to andrographolide (1.4, 2.8, and 5.6 µM) and pioglitazone (0.02 µM). The results are shown as mean values ± SE (n=3). A, Andrographolide; Pio, Pioglitazone 0.02 µM. $^*p < 0.05$ indicates a statistically significant difference in comparison to that of control cells.

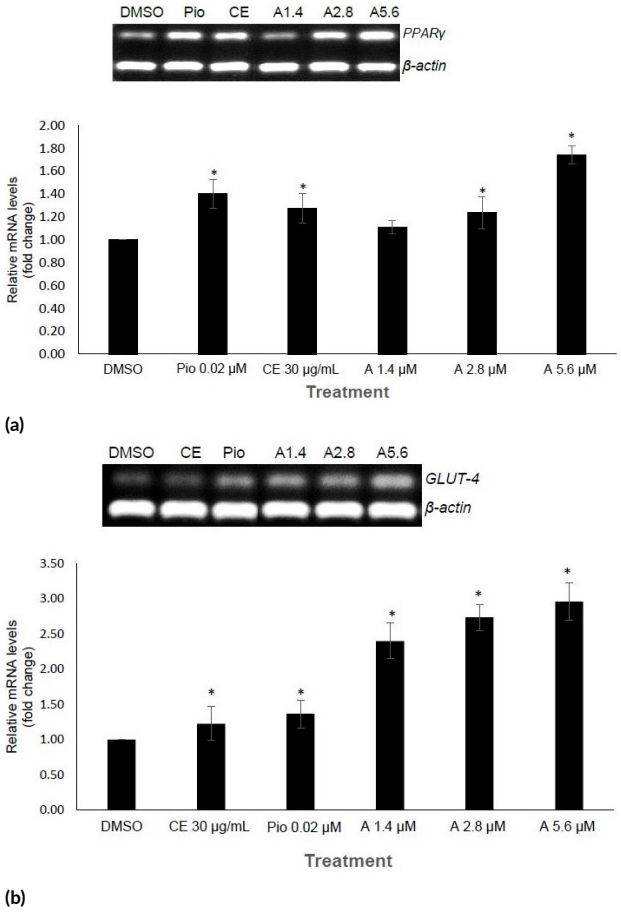

FIGURE 4 Effect of andrographolide on gene expression. (a) *PPARγ* mRNA levels after treatments in mature adipocytes. (b) GLUT-4 mRNA levels after treatments in mature adipocytes. The results are shown as mean values ± SE (n=3). A, Andrographolide (1.4, 2.8 and 5.6 µM); Pio, Pioglitazone 0.02 µM; CE, Crude extract 30 mg/mL. $^*p < 0.05$ indicates a statistically significant difference compared to that of DMSO (control).

more, upregulated *PPARγ* can enhance insulin sensitivity by increasing the number of adipocytes and the expression of genes such as adiponectin and *GLUT-4* (Anusree et al. 2014).

Our study demonstrated that administration of andrographolide over time increases glucose uptake ability, dependent on the concentration. Consequently, the glucose uptake effect of andrographolide in this study predicted that *PPARγ* upregulation in mature adipocytes might enhance *GLUT-4* expression. The study shows that andrographolide enhances the expression of *PPARγ* and *GLUT-4* on mRNA levels in mature adipocytes similar to or even greater than pioglitazone. As a result, andrographolide may have the same action as pioglitazone to increase cellular glucose uptake and insulin sensitivity; thus, it can be used as an alternative therapy for type 2 DM. This study is expected to add to existing research on *A. paniculata* and aid in understanding the antidiabetic effect of a single isolated andrographolide from this herb.

4. Conclusions

In the study, andrographolide isolated from sambiloto herbs (*A. paniculata* (Burm.f.) Nees) was exhibited to improve the glucose uptake on 3T3-L1 adipocytes by increasing *PPARγ* and *GLUT-4* expression, thus, it has the potential to develop as an antidiabetic therapeutic agent.

Acknowledgments

We thank Dexa Laboratories of Biomolecular Sciences (DLBS) for the provision of research facilities. Great appreciation is also addressed to the UGM Research Directorate through the ”2019 Research Assistance Program Grant” for the financial support of the research.

Authors' contributions

NTA, PRN, RT, AEN, SP designed the study. NTA, PRN, SP carried out the laboratory work. NTA, PRN analyzed the data. NTA, AEN wrote the manuscript. All authors read and approved the final version of the manuscript.

Competing interests

The authors declare that they have no competing interest.

References

Ahmadian M, Suh JM, Hah N, Liddle C, Atkins AR, Downes M, Evans RM. 2013. *PPARγ* signaling and metabolism: The good, the bad and the future. Nat. Med. 19(5):557–566. doi:10.1038/nm.3159.

Al-Goblan AS, Al-Alfi MA, Khan MZ. 2014. Mechanism linking diabetes mellitus and obesity. Diabetes, Metab. Syndr. Obes. Targets Ther. 7:587—591. doi:10.2147/DMSO.S67400.

Anusree SS, Priyanka A, Nisha VM, Das AA, Raghu KG. 2014. An *in vitro* study reveals the nutraceutical potential of punicic acid relevant to diabetes via enhanced *GLUT4* expression and adiponectin secretion. Food Funct. 5(10):2590–2601. doi:10.1039/c4fo00302k.

Bao S, Wu YL, Wang X, Han S, Cho SB, Ao W, Nan JX. 2020. Agriophyllum oligosaccharides ameliorate hepatic injury in type 2 diabetic db/db mice targeting INS-R/IRS-2/PI3K/AKT/*PPAR-γ/GLUT4* signal pathway. J. Ethnopharmacol. 257:112863. doi:10.1016/j.jep.2020.112863.

Basu A, Jensen MD, McCann F, Mukhopadhyay D, Joyner MJ, Rizza RA. 2006. Effects of pioglitazone versus glipizide on body fat distribution, body water content, and hemodynamics in type 2 diabetes. Diabetes Care 29(3):510–514. doi:10.2337/diacare.29.03.06.dc05-2004.

Blanchard PG, Turcotte V, Côté M, Gélinas Y, Nilsson S, Olivecrona G, Deshaies Y, Festuccia WT. 2016. Peroxisome proliferator-activated receptor γ activation favours selective subcutaneous lipid deposition by coordinately regulating lipoprotein lipase modulators, fatty acid transporters and lipogenic enzymes. Acta Physiol. 217(3):227–239. doi:10.1111/apha.12665.

Cao H, Graves DJ, Anderson RA. 2010. Cinnamon extract regulates glucose transporter and insulin-signaling gene expression in mouse adipocytes. Phytomedicine 17(13):1027–1032. doi:10.1016/j.phymed.2010.03.023.

Chait A, den Hartigh LJ. 2020. Adipose tissue distribution, inflammation and its metabolic consequences, including diabetes and cardiovascular disease. Front. Cardiovasc. Med. 7:22. doi:10.3389/fcvm.2020.00022.

Cignarelli A, Giorgino F, Vettor R. 2013. Pharmacologic agents for type 2 diabetes therapy and regulation of adipogenesis. Arch. Physiol. Biochem. 119(4):139–150. doi:10.3109/13813455.2013.796996.

Fajas L. 2003. Adipogenesis: A cross-talk between cell proliferation and cell differentiation. Ann. Med. 35(2):79–85. doi:10.1080/07853890310009999.

Fajrin FA, Nugroho AE, Nurrochmad A, Susilowati R. 2020. Ginger extract and its compound, 6-shogaol, attenuates painful diabetic neuropathy in mice via reducing *TRPV1* and *NMDAR2B* expressions in the spinal cord. J. Ethnopharmacol. 249:112396. doi:10.1016/j.jep.2019.112396.

Fan Y, Gan M, Tan Y, Chen L, Shen L, Niu L, Liu Y, Tang G, Jiang Y, Li X, Zhang S, Bai L, Zhu L. 2019. MiR-152 regulates 3T3-L1 preadipocyte proliferation and differentiation. Molecules 24(18):3379. doi:10.3390/molecules24183379.

Fasshauer M, Klein J, Ueki K, Kriauciunas KM, Benito M, White MF, Kahn CR. 2000. Essential role of insulin receptor substrate-2 in insulin stimulation of *GLUT4* translocation and glucose uptake in brown adipocytes. J. Biol. Chem. 275(33):25494–25501. doi:10.1074/jbc.M004046200.

Fitrawan LO, Ariastuti R, Tjandrawinata R, Nugroho A, Pramono S. 2018. Antidiabetic effect of combination of fractionated-extracts of *Andrographis paniculata* and *Centella asiatica*: *In vitro* study. Asian Pac. J. Trop. Biomed. 8(11):527–532. doi:10.4103/2221-1691.245957.

Fu Y, Luo N, Klein RL, Timothy Garvey W. 2005. Adiponectin promotes adipocyte differentiation, insulin sensitivity, and lipid accumulation. J. Lipid Res. 46(7):1369–1379. doi:10.1194/jlr.M400373-JLR200.

Gandhi GR, Stalin A, Balakrishna K, Ignacimuthu S, Paulraj MG, Vishal R. 2013. Insulin sensitization via partial agonism of *PPARγ* and glucose uptake through translocation and activation of *GLUT4* in PI3K/p-Akt signaling pathway by embelin in type 2 diabetic rats. Biochim. Biophys. Acta - Gen. Subj. 1830(1):2243–2255. doi:10.1016/j.bbagen.2012.10.016.

Harwoko, Pramono S, Nugroho AE. 2014. Triterpenoid-rich fraction of *Centella asiatica* leaves and in vivo antihypertensive activity. Int. Food Res. J. 21(1):149–154. URL http://www.ifrj.upm.edu.my/21%20(01)%202014/21%20IFRJ%2021%20(01)%202014%20Agung%20388.pdf.

Hauner H. 2002. The mode of action of thiazolidinediones. Diabetes. Metab. Res. Rev. 18(S2):S10–S15. doi:10.1002/dmrr.249.

Horita S, Nakamura M, Satoh N, Suzuki M, Seki G. 2015. Thiazolidinediones and edema: Recent advances in the pathogenesis of Thiazolidinediones-induced renal sodium retention. doi:10.1155/2015/646423.

Jin L, Fang W, Li B, Shi G, Li X, Yang Y, Yang J, Zhang Z, Ning G. 2012. Inhibitory effect of Andrographolide in 3T3-L1 adipocytes differentiation through the *PPARγ* pathway. Mol. Cell. Endocrinol. 358(1):81–87. doi:10.1016/j.mce.2012.02.025.

Jin L, Shi G, Ning G, Li X, Zhang Z. 2011. Andrographolide attenuates tumor necrosis factor-alpha-induced insulin resistance in 3T3-L1 adipocytes. Mol. Cell. Endocrinol. 332(1-2):134–139. doi:10.1016/j.mce.2010.10.005.

Kvandová M, Majzúnová M, Dovinová I. 2016. The role of *PPARγ* in cardiovascular diseases. Physiol. Res. 65(Suppl. 3):S343–S363. doi:10.33549/physiolres.933439.

Lefterova MI, Zhang Y, Steger DJ, Schupp M, Schug J, Cristancho A, Feng D, Zhuo D, Stoeckert CJ, Liu XS, Lazar MA. 2008. *PPARγ* and *C/EBP* factors orchestrate adipocyte biology via adjacent binding on a

genome-wide scale. Genes Dev. 22(21):2941–2952. doi:10.1101/gad.1709008.

Maiti K, Mukherjee K, Murugan V, Saha BP, Mukherjee PK. 2010. Enhancing bioavailability and hepatoprotective activity of andrographolide from *Andrographis paniculata*, a well-known medicinal food, through its herbosome. J. Sci. Food Agric. 90(1):43–51. doi:10.1002/jsfa.3777.

Malik Z, Parveen R, Parveen B, Zahiruddin S, Aasif Khan M, Khan A, Massey S, Ahmad S, Husain SA. 2021. Anticancer potential of andrographolide from *Andrographis paniculata* (Burm.f.) Nees and its mechanisms of action. J. Ethnopharmacol. 272:113936. doi:10.1016/j.jep.2021.113936.

Moseti D, Regassa A, Kim WK. 2016. Molecular regulation of adipogenesis and potential anti-adipogenic bioactive molecules. Int. J. Mol. Sci. 17(1):124. doi:10.3390/ijms17010124.

Novitasari PR, Astuti NT, Pramono S, Tjandrawinata R, Nugroho AE. 2020. A simple Liquid-Liquid Fractionation (LLF) method for isolating deoxyandrographolide dan andrographolide from herbs of *Andrographis paniculata* (Burm., F) Ness and its cytotoxic activity on 3T3-L1 preadipocyte cells. J. Food Pharm. Sci. 8(3):306–314. doi:10.22146/jfps.875.

Nugroho AE, Anas Y, Arsito PN, Wibowo JT, Riyanto S, Sukari MA. 2011. Effects of marmin, a compound isolated from Aegle marmelos correa, on contraction of the guinea pig-isolated trachea. Pak. J. Pharm. Sci. 24(4):427–33.

Nugroho AE, Andrie M, Warditiani NK, Siswanto E, Pramono S, Lukitaningsih E. 2012. Antidiabetic and antihiperlipidemic effect of *Andrographis paniculata* (Burm. f.) Nees and andrographolide in high-fructose-fat-fed rats. Indian J. Pharmacol. 44(3):377–381. doi:10.4103/0253-7613.96343.

Nugroho AE, Rais IR, Setiawan I, Pratiwi PY, Hadibarata T, Tegar M, Pramono S. 2013. Pancreatic effect of andrographolide isolated from *Andrographis paniculata* (Burm. f.) Nees. Pakistan J. Biol. Sci. 17(1):22–31. doi:10.3923/pjbs.2014.22.31.

Pereira AS, Banegas-Luna AJ, Peña-García J, Pérez-Sánchez H, Apostolides Z. 2019. Evaluation of the anti-diabetic activity of some common herbs and spices: Providing new insights with inverse virtual screening. Molecules 24(22):4030. doi:10.3390/molecules24224030.

Rafat A, Philip K, Muniandy S. 2010. Antioxidant potential and content of phenolic compounds in ethanolic extracts of selected parts of *Andrographis paniculata*. J. Med. Plants Res. 4(3):197–202. URL https://academicjournals.org/article/article1380378955_Arash%20et%20al.pdf.

Sarjeant K, Stephens JM. 2012. Adipogenesis. Cold Spring Harb. Perspect Biol. 4:a008417. doi:10.1101/cshperspect.a008417.

Shoelson SE, Lee J, Goldfine AB. 2006. Inflammation and insulin resistance. J. Clin. Invest. 116(7):1793–1801. doi:10.1172/JCI29069.

Soccio RE, Chen ER, Lazar MA. 2014. Thiazolidinediones and the promise of insulin sensitization in type 2 diabetes. Cell Metab. 20(4):573–591. doi:10.1016/j.cmet.2014.08.005.

Sugii S, Olson P, Sears DD, Saberi M, Atkins AR, Barish GD, Hong SH, Castro GL, Yin YQ, Nelson MC, Hsiao G, Greaves DR, Downes M, Yu RT, Olefsky JM, Evans RM. 2009. *PPARγ* activation in adipocytes is sufficient for systemic insulin sensitization. Proc. Natl. Acad. Sci. U. S. A. 106(52):22504–22509. doi:10.1073/pnas.0912487106.

Tjandrawinata RR, Wulan DD, Nailufar F, Sinambela J, Tandrasasmita OM. 2011. Glucose-lowering effect of DLBS3233 is mediated through phosphorylation of tyrosine and upregulation of *PPARγ* and *GLUT4* expression. Int. J. Gen. Med. 4:345–357. doi:10.2147/IJGM.S16517.

Wang S, Dougherty EJ, Danner RL. 2016. *PPARγ* signaling and emerging opportunities for improved therapeutics. Pharmacol. Res. 111:76–85. doi:10.1016/j.phrs.2016.02.028.

Widyawaruyanti A, Asrory M, Ekasari W, Setiawan D, Radjaram A, Tumewu L, Hafid AF. 2014. *In vivo* antimalarial activity of *Andrographis paniculata* tablets. Procedia Chem. 13:101–104. doi:10.1016/j.proche.2014.12.012.

Wigati D, Anwar K, Sudarsono, Nugroho AE. 2017. Hypotensive activity of ethanolic extracts of *Morinda citrifolia* L. leaves and fruit in dexamethasone-induced hypertensive rat. J. Evidence-Based Complement. Altern. Med. 22(1):101–104. doi:10.1177/2156587216653660.

Zheng Y, Ley SH, Hu FB. 2018. Global aetiology and epidemiology of type 2 diabetes mellitus and its complications. Nat. Rev. Endocrinol. 14(2):101–104. doi:10.1038/nrendo.2017.151.